

# Hot-pressed, dry, composite, PEO-based electrolyte membranes

## I. Ionic conductivity characterization

G.B. Appetecchi<sup>a</sup>, F. Croce<sup>a</sup>, J. Hassoun<sup>a</sup>, B. Scrosati<sup>a</sup>,  
Mark Salomon<sup>b,\*</sup>, Frank Cassel<sup>b</sup>

<sup>a</sup>University of Rome "La Sapienza", Piazzale Aldo Moro 5, 00185 Roma, Italy

<sup>b</sup>MaxPower Inc., 220 Stahl Road, Harleysville, PA 19438, USA

Received 14 September 2002; accepted 26 September 2002

### Abstract

Lithium polymer composite electrolytes, formed by a blend of poly(ethylene oxide) (PEO), LiCF<sub>3</sub>SO<sub>3</sub> lithium salt and a selected, nanoparticle ceramic filler, were prepared by hot-pressing through a solvent-free procedure. These dry, ionically conducting membranes were characterized in terms of ionic conductivity in the 30–105 °C temperature range. The influences of several parameters such as the temperature, PEO molecular mass, the EO/Li molar ratio, and the nature and the content of ceramic filler were carefully evaluated.

© 2002 Elsevier Science B.V. All rights reserved.

**Keywords:** Poly(ethylene oxide); Dry polymer electrolyte; Solvent-free preparation; Hot-pressing; Solid-state electrolytes; Composite electrolytes; Conductivity

### 1. Introduction

Poly(ethylene oxide) (PEO)-based lithium electrolyte membranes appear the most suitable candidates as separators for reliable, lithium rechargeable polymer batteries [1–3]. These membranes are formed by dissolving a lithium salt, e.g. LiClO<sub>4</sub>, LiCF<sub>3</sub>SO<sub>3</sub>, etc. in a PEO polymer matrix to form a solid, lithium ion conductor [4]. Nevertheless, the PEO–LiX complexes perform well in terms of ionic conductivity only when the polymer is in its amorphous state, i.e. under the condition of relatively poor mechanical stability. Wiczorek et al. [5] proposed to improve the mechanical properties of the polymer electrolyte by the dispersion of ceramic powders in its bulk. Other authors [6,7] showed that the ionic conductivity may also be enhanced by the addition of a ceramic filler. It has also been shown [8,9] that the particle size of the filler plays an important role in improving the properties of the polymer electrolyte. Recent work [10–14] demonstrated the feasibility of a more rapid and less expensive solvent-free procedure (i.e. hot pressing, extrusion) for the preparation of totally dry membranes.

In this paper, we report the synthesis and the characterization in terms of ionic conductivity of PEO-based, ceramic-added composite, polymer electrolytes prepared by hot-pressing through a solvent-free procedure. Several P(EO)<sub>n</sub>-LiCF<sub>3</sub>SO<sub>3</sub>-ceramic filler compositions were examined. In particular, the investigation is focused on the effect of (i) temperature, (ii) the PEO molecular mass, (iii) the EO/Li molar ratio, (iv) the nature and the content of filler. Nanoscale Al<sub>2</sub>O<sub>3</sub> and SiO<sub>2</sub> were selected as the ceramic fillers.

### 2. Experimental

#### 2.1. Composite membranes preparation

The PEO-based, composite polymer electrolyte membranes were prepared following a solvent-free procedure [10,11]. Linear poly(ethylene oxide), PEO (Aldrich), having a molecular mass (hereafter MW) ranging from 1 × 10<sup>5</sup> to 6 × 10<sup>5</sup>, was dried under vacuum at 60 °C for 24 h before use. Nanoscale (<7 nm) fumed SiO<sub>2</sub> (Aldrich) and Al<sub>2</sub>O<sub>3</sub> (Aldrich) fillers were dried under vacuum at 300 °C for 24 h. LiCF<sub>3</sub>SO<sub>3</sub> (Aldrich, Battery Grade product having a water content lower than 20 ppm) was used as received. The electrolyte components (i.e. PEO polymer, lithium salt and ceramic filler) were carefully sieved and only the

\* Corresponding author. Tel.: +1-215-513-4230/4231;

fax: +1-215-513-4232.

E-mail address: msalomon@monmouth.com (M. Salomon).

Table 1

Composition of the hot-pressed, nanocomposite, PEO-based electrolyte membranes of Series I (PEO molecular mass = 100,000), Series II (300,000) and Series III (600,000), respectively

EO/Li molar ratio	Al <sub>2</sub> O <sub>3</sub> filler		SiO <sub>2</sub> filler	
	5 wt. %	10 wt. %	5 wt. %	10 wt. %
Series I (PEO MW = 100,000)				
20	Membrane I-1	Membrane I-2	Membrane I-3	Membrane I-4
35	Membrane I-5	Membrane I-6	Membrane I-7	Membrane I-8
50	Membrane I-9	Membrane I-10	Membrane I-11	Membrane I-12
Series II (PEO MW = 300,000)				
20	–	–	Membrane II-3	–
35	–	–	Membrane II-7	–
50	–	–	Membrane II-11	–
Series III (PEO MW = 600,000)				
20	Membrane III-1	Membrane III-2	Membrane III-3	Membrane III-4
35	Membrane III-5	Membrane III-6	Membrane III-7	Membrane III-8
50	Membrane III-9	Membrane III-10	Membrane III-11	Membrane III-12

EO/Li ratio: 20, 35, 50. Filler type: Al<sub>2</sub>O<sub>3</sub>, SiO<sub>2</sub>. Filler content: 5 and 10 wt. %.

smallest particle size fractions were used. The sieved and dried components were introduced in their right proportion inside sealed, polyethylene bottles and were intimately mixed by ball-milling for at least 24 h to obtain a homogeneous mixture of the powders. The mixtures were then hot-pressed in an aluminum mold using a temperature and a pressure (depending on the PEO molecular weight) ranging from 70 to 80 °C and from 3 to 4 tons, respectively. The mixtures were processed from 10 to 20 min. Finally, the polymer electrolyte membranes were stored under argon.

This procedure resulted in very homogeneous, semi-transparent, composite membranes having very good mechanical strength. The surface area and the thickness ranged from 30 to 50 cm<sup>2</sup> and from 100 to 150 μm, respectively. Any contamination with the external air was carefully avoided since all preparation steps were performed in a controlled, argon-atmosphere environment (dry-box) having a humidity content below 10 ppm. For those processes (e.g. sieving, mixing, hot-pressing) which required operation in the open air, the materials were first housed in sealed, coffee-bag

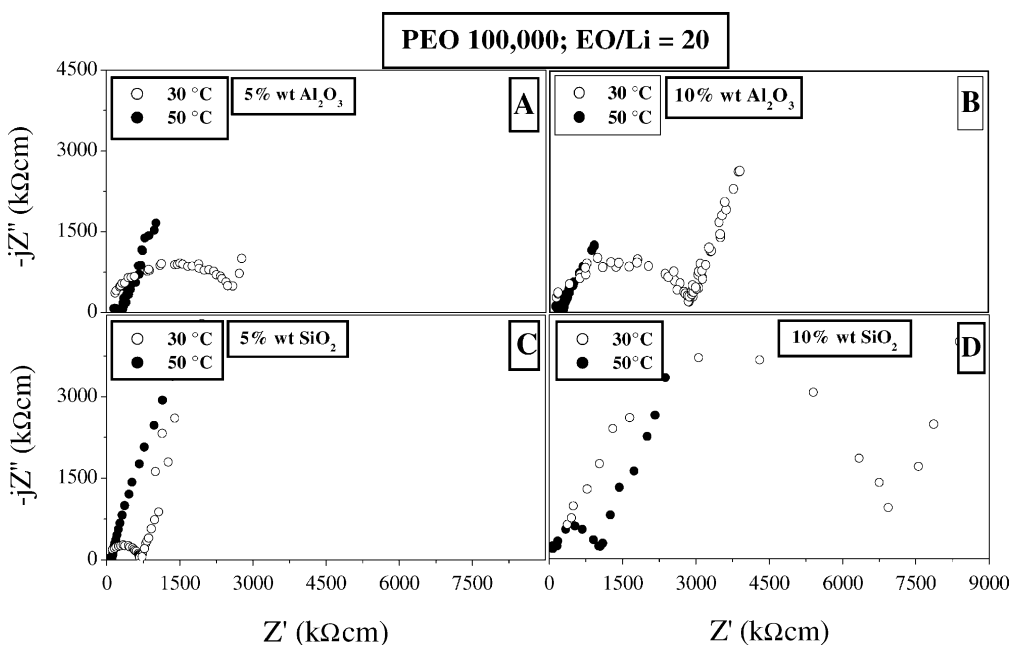


Fig. 1. Selected, normalized impedance responses of hot-pressed, nanocomposite, P(EO)<sub>20</sub>LiCF<sub>3</sub>SO<sub>3</sub> for Series I electrolyte membranes as a function of wt. % filler. Frequency range: 100 kHz–1 Hz. Temperature range: 30–50 °C and PEO molecular mass = 100,000. Panels from A to D refer to filler contents of 5 wt. % Al<sub>2</sub>O<sub>3</sub> (panel A), 10 wt. % Al<sub>2</sub>O<sub>3</sub> (panel B), 5 wt. % SiO<sub>2</sub> (panel C) and 10 wt. % SiO<sub>2</sub> (panel D), respectively.

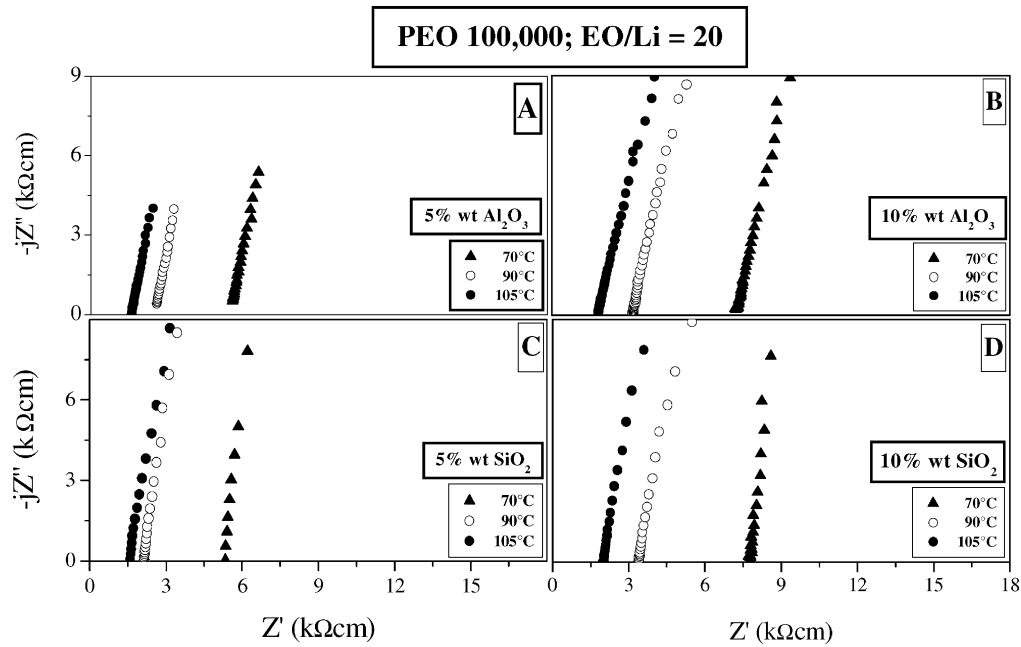


Fig. 2. Selected, normalized impedance responses of hot-pressed, nanocomposite,  $\text{P}(\text{EO})_{20}\text{LiCF}_3\text{SO}_3$  for Series I electrolyte membranes. Frequency range: 100 kHz–1 Hz. Temperature range: 70–105 °C. PEO molecular mass = 100,000, and panels A to D refer to filler contents of 5 wt.%  $\text{Al}_2\text{O}_3$  (panel A), 10 wt.%  $\text{Al}_2\text{O}_3$  (panel B), 5 wt.%  $\text{SiO}_2$  (panel C) and 10 wt.%  $\text{SiO}_2$  (panel D), respectively.

envelopes and, then, removed from the dry-box for being processed. Following this procedure, three series of hot-pressed, dry, composite membranes, differing by the MWs of the PEO component, the EO/Li molar ratio and the nature and the filler content, were prepared. The compositions of the three membrane series (coded Series I, II and III, respectively) are listed in Table 1.

## 2.2. Ionic conductivity measurements

The ionic conductivity of all membranes was determined by AC impedance spectroscopy. Cells using two blocking, stainless steel electrodes were used to hold the membrane sample. A Teflon spacer was included to fix the sample thickness. The cells were assembled in a controlled, argon-

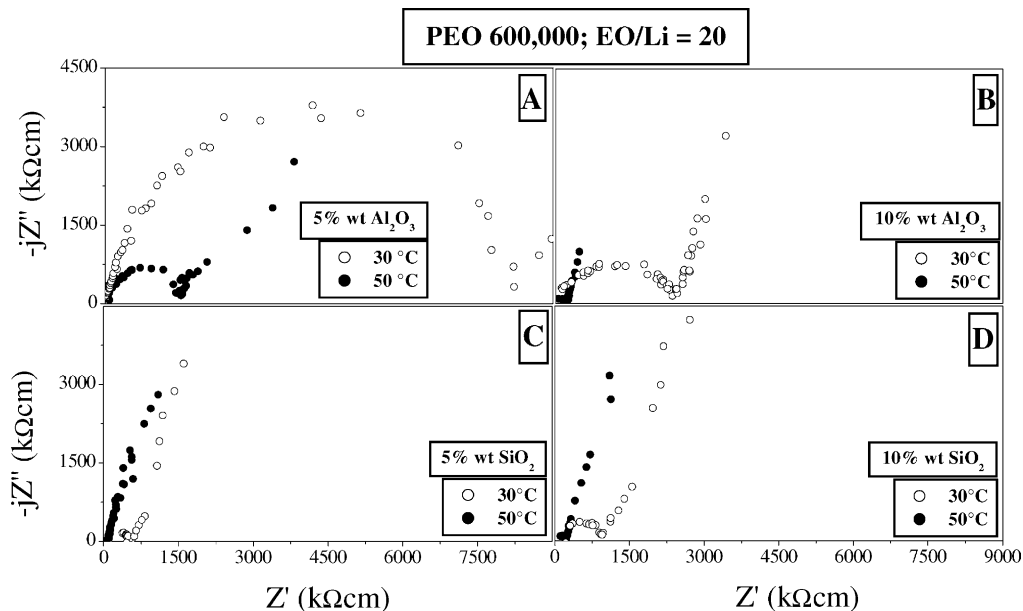


Fig. 3. Selected, normalized impedance responses of hot-pressed, nanocomposite,  $\text{P}(\text{EO})_{20}\text{LiCF}_3\text{SO}_3$  for Series III electrolyte membranes. Frequency range: 100 kHz–1 Hz. Temperature range: 30–50 °C. PEO molecular mass = 600,000. Panels A to D refer to filler contents of 5 wt.%  $\text{Al}_2\text{O}_3$  (panel A), 10 wt.%  $\text{Al}_2\text{O}_3$  (panel B), 5 wt.%  $\text{SiO}_2$  (panel C) and 10 wt.%  $\text{SiO}_2$  (panel D), respectively.

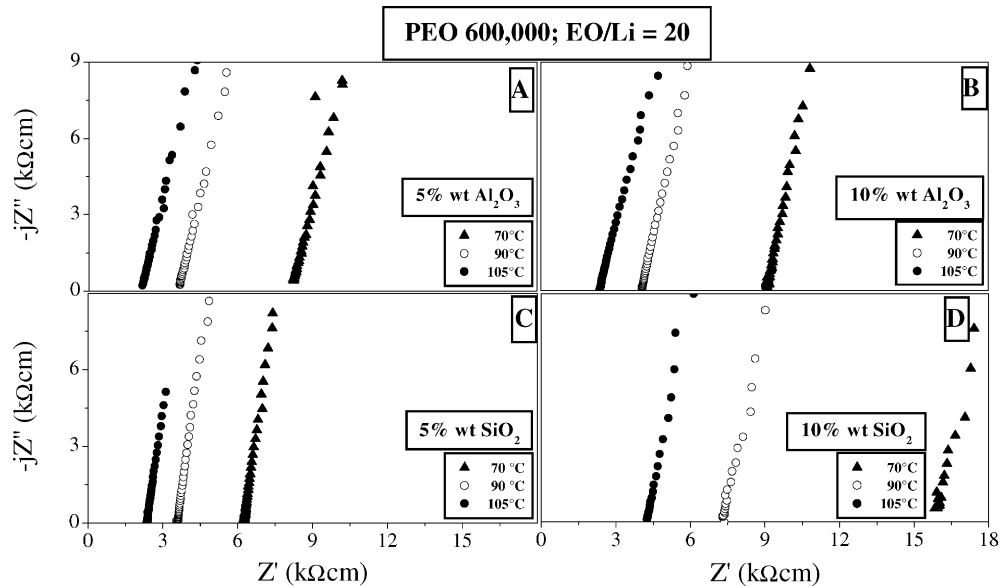


Fig. 4. Selected, normalized impedance responses of hot-pressed, nanocomposite,  $P(\text{EO})_{20}\text{LiCF}_3\text{SO}_3$  for Series III electrolyte membranes. Frequency range: 100 kHz–1 Hz. Temperature range: 70–105 °C. PEO molecular mass = 600,000. Panels A to D refer to filler contents of 5 wt.%  $\text{Al}_2\text{O}_3$  (panel A), 10 wt.%  $\text{Al}_2\text{O}_3$  (panel B), 5 wt.%  $\text{SiO}_2$  (panel C) and 10 wt.%  $\text{SiO}_2$  (panel D), respectively.

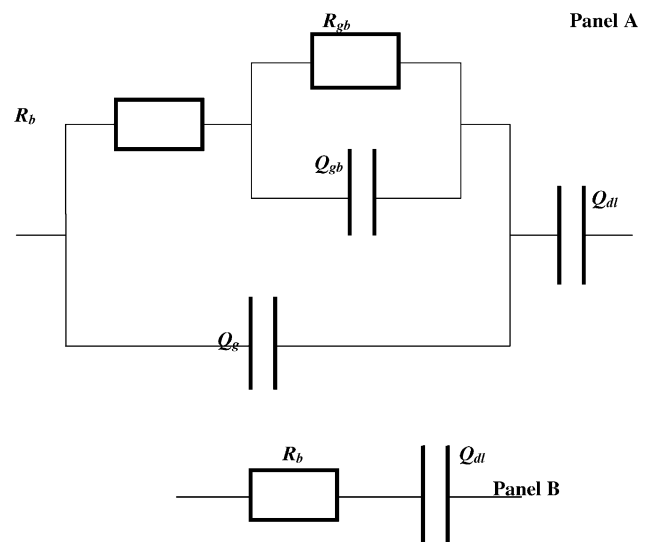
filled dry-box (MBRAUN LabMaster 130) having humidity and oxygen contents below 1 ppm. The cells were housed in sealed, coffee-bag envelopes and, then, removed from the dry-box for the tests. Initially, the cells were heated to 105 °C and kept at this temperature for at least 12 h to reach thermal equilibrium and then conductivities were measured at different intervals (i.e. every 15–20 °C by a cooling scan) in the 105–30 °C temperature range. For each temperature, the final conductivity value was taken when no change of the shape of the AC impedance response was detected. Temperature control was provided by a forced air oven. The impedance tests were carried out in the 65 kHz–1 Hz frequency range using a Frequency Response Analyzer (FRA), Schlumberger Solartron model 1260 coupled with a Schlumberger Solartron model 1286 Electrochemical Interface.

### 3. Results and discussion

#### 3.1. Impedance measurements

Figs. 1–4 show the AC impedance response of Series I electrolyte membranes (see Table 1) in two temperature ranges, i.e. from 30 to 50 °C and from 70 to 105 °C, respectively. Panels from A to D of each figure are referred to different types and/or contents of the ceramic filler, i.e. 5 wt.%  $\text{Al}_2\text{O}_3$  (panel A), 10 wt.%  $\text{Al}_2\text{O}_3$  (panel B), 5 wt.%  $\text{SiO}_2$  (panel C) and 10 wt.%  $\text{SiO}_2$  (panel D). All impedance spectra were normalized to account for the area and the thickness of the sample membrane. At low–medium temperatures ( $\leq 50$  °C, Figs. 1 and 3), the composite PEO membranes exhibit the typical impedance response of a polymer electrolyte sandwiched between two quasi-blocking

electrodes [15]. A semicircle is observed at medium–high frequencies (100 kHz–100 Hz). This semicircle has an asymmetric shape, as the result of the convolution of two different contributes, i.e. bulk and grain boundary [15], to the ionic resistance of the electrolyte membrane. An inclined



#### Legend:

- $R_b$  = bulk ionic resistance
- $R_{gb}$  = grain boundary resistance
- $Q_g$  = geometric CPE
- $Q_{gb}$  = grain boundary CPE
- $Q_{dl}$  = double layer CPE

Fig. 5. General equivalent circuit model (panel A) proposed for the analysis of the impedance measurements of the hot-pressed, nanocomposite, PEO-based, polymer electrolyte membranes of the Series I, II and III. Simplified circuit (panel B) used for the NLLSQ fit of the AC responses taken at medium–high temperatures.

straight line towards the real axes,  $Z'$ , typical of blocking electrode capacitive behavior [15] (electrolyte/electrode double layer capacitance), is observed at low frequencies. At medium–high temperatures ( $\geq 70$  °C, Figs. 2 and 4), the semicircle disappears as a result of its shift to higher frequencies due to the decrease of the ionic resistance of the electrolyte. The plots are consistent in showing an inclined straight line whose intercept with the real axes gives the PEO membrane's ionic conductivity [15]. A progressive shift towards the axes origin of the high frequency intercept is noticed with temperature increase, reveals a corresponding enhancement of the ionic conductivity.

### 3.2. Analysis of AC responses

The analysis of the impedance responses was performed using a common approach, i.e. by defining an equivalent circuit taking into account all possible contributors to the impedance of the tested electrolyte membranes [15]. The validity of the chosen circuit was confirmed by fitting the impedance responses using a Non-Linear Least-Square

(NLLSQ) fit software developed by Boukamp [16,17]. Only fits characterized by a  $\chi^2$  factor [16,17] lower than  $10^{-4}$  were considered acceptable to insure the validity of the proposed model. The general equivalent circuit proposed to represent the electrochemical cell here under study is depicted in Fig. 5, panel A. This circuit takes into account both the bulk ( $R_b$ ) and the grain boundary ( $R_{gb}$ ) contributions to the total resistance of the PEO electrolyte membrane. A constant-phase element, CPE ( $Q$ ), was used in the place of pure capacitance ( $C$ ). The  $Q_g$  and  $Q_{gb}$  (in parallel with  $R_{gb}$ ) elements are related to the geometric and to the grain boundary capacitance, respectively. Finally, the  $Q_{dl}$  element takes into account the double layer capacitance at the electrolyte/electrode interface. At medium–high temperatures ( $\geq 70$  °C), a substantial modification of the shape of the AC responses occurs: no grain boundary contribution is observed and the geometric capacitance is not detected because of the temperature effect (see Figs. 2 and 4). Therefore, the impedance measurements can be properly fitted by a simplified version of the equivalent circuit, i.e. by a circuit only formed by the  $R_b$  and  $Q_{dl}$  elements in series (panel B).

Table 2

Ionic conductivity values of the hot-pressed, nanocomposite, PEO-based electrolyte membranes of the Series I, II and III at different temperatures (30–105 °C)

Membrane sample	Ionic conductivity ( $S\ cm^{-1}$ )				
	30 °C	50 °C	70 °C	90 °C	105 °C
Series I					
I-1	$3.8 \times 10^{-7}$	$3.9 \times 10^{-6}$	$1.8 \times 10^{-4}$	$4.0 \times 10^{-4}$	$6.2 \times 10^{-4}$
I-2	$3.6 \times 10^{-7}$	$4.1 \times 10^{-6}$	$1.4 \times 10^{-4}$	$3.2 \times 10^{-4}$	$5.6 \times 10^{-4}$
I-3	$1.3 \times 10^{-6}$	$9.7 \times 10^{-6}$	$2.1 \times 10^{-4}$	$4.5 \times 10^{-4}$	$6.1 \times 10^{-4}$
I-4	$8.4 \times 10^{-8}$	$1.7 \times 10^{-6}$	$1.3 \times 10^{-4}$	$3.0 \times 10^{-4}$	$5.1 \times 10^{-4}$
I-5	$3.1 \times 10^{-7}$	$3.5 \times 10^{-6}$	$2.9 \times 10^{-4}$	$4.7 \times 10^{-4}$	$6.1 \times 10^{-4}$
I-6	$4.0 \times 10^{-7}$	$4.3 \times 10^{-6}$	$2.4 \times 10^{-4}$	$3.7 \times 10^{-4}$	$4.8 \times 10^{-4}$
I-7	$1.8 \times 10^{-6}$	$8.6 \times 10^{-6}$	$3.0 \times 10^{-4}$	$4.7 \times 10^{-4}$	$6.0 \times 10^{-4}$
I-8	$7.1 \times 10^{-7}$	$6.4 \times 10^{-6}$	$2.6 \times 10^{-4}$	$4.0 \times 10^{-4}$	$5.1 \times 10^{-4}$
I-9	$2.5 \times 10^{-7}$	$3.4 \times 10^{-6}$	$2.0 \times 10^{-4}$	$3.0 \times 10^{-4}$	$3.8 \times 10^{-4}$
I-10	$3.0 \times 10^{-6}$	$3.5 \times 10^{-5}$	$1.9 \times 10^{-4}$	$2.8 \times 10^{-4}$	$3.3 \times 10^{-4}$
I-11	$8.7 \times 10^{-7}$	$6.9 \times 10^{-6}$	$2.3 \times 10^{-4}$	$3.8 \times 10^{-4}$	$4.6 \times 10^{-4}$
I-12	$8.1 \times 10^{-7}$	$6.8 \times 10^{-6}$	$2.4 \times 10^{-4}$	$3.6 \times 10^{-4}$	$4.7 \times 10^{-4}$
Series II					
II-3	$4.8 \times 10^{-7}$	$3.2 \times 10^{-6}$	$1.1 \times 10^{-4}$	$2.5 \times 10^{-4}$	$4.3 \times 10^{-4}$
II-7	$1.1 \times 10^{-6}$	$9.5 \times 10^{-6}$	$1.4 \times 10^{-4}$	$2.9 \times 10^{-4}$	$4.4 \times 10^{-4}$
II-11	$8.9 \times 10^{-7}$	$6.5 \times 10^{-6}$	$2.4 \times 10^{-4}$	$3.9 \times 10^{-4}$	$4.7 \times 10^{-4}$
Series III					
III-1	$6.7 \times 10^{-8}$	$7.0 \times 10^{-7}$	$1.2 \times 10^{-4}$	$2.8 \times 10^{-4}$	$4.8 \times 10^{-4}$
III-2	$4.5 \times 10^{-7}$	$4.7 \times 10^{-6}$	$1.1 \times 10^{-4}$	$2.5 \times 10^{-4}$	$4.3 \times 10^{-4}$
III-3	$1.9 \times 10^{-6}$	$1.3 \times 10^{-5}$	$1.6 \times 10^{-4}$	$2.8 \times 10^{-4}$	$4.2 \times 10^{-4}$
III-4	$2.1 \times 10^{-6}$	$8.8 \times 10^{-6}$	$1.1 \times 10^{-4}$	$2.2 \times 10^{-4}$	$3.9 \times 10^{-4}$
III-5	$1.7 \times 10^{-7}$	$2.0 \times 10^{-6}$	$2.3 \times 10^{-4}$	$3.8 \times 10^{-4}$	$4.8 \times 10^{-4}$
III-6	$5.5 \times 10^{-7}$	$6.0 \times 10^{-6}$	$1.7 \times 10^{-4}$	$4.0 \times 10^{-4}$	$5.1 \times 10^{-4}$
III-7	$5.8 \times 10^{-7}$	$4.9 \times 10^{-6}$	$1.2 \times 10^{-4}$	$2.5 \times 10^{-4}$	$3.5 \times 10^{-4}$
III-8	$9.9 \times 10^{-7}$	$8.2 \times 10^{-6}$	$1.4 \times 10^{-4}$	$3.1 \times 10^{-4}$	$4.0 \times 10^{-4}$
III-9	$9.1 \times 10^{-7}$	$7.9 \times 10^{-6}$	$1.8 \times 10^{-4}$	$2.7 \times 10^{-4}$	$3.4 \times 10^{-4}$
III-10	$1.7 \times 10^{-6}$	$1.2 \times 10^{-5}$	$2.0 \times 10^{-4}$	$2.7 \times 10^{-4}$	$2.9 \times 10^{-4}$
III-11	$8.2 \times 10^{-7}$	$7.0 \times 10^{-6}$	$1.7 \times 10^{-4}$	$2.5 \times 10^{-4}$	$3.1 \times 10^{-4}$
III-12	$1.0 \times 10^{-6}$	$1.1 \times 10^{-5}$	$1.5 \times 10^{-4}$	$2.1 \times 10^{-4}$	$2.6 \times 10^{-4}$

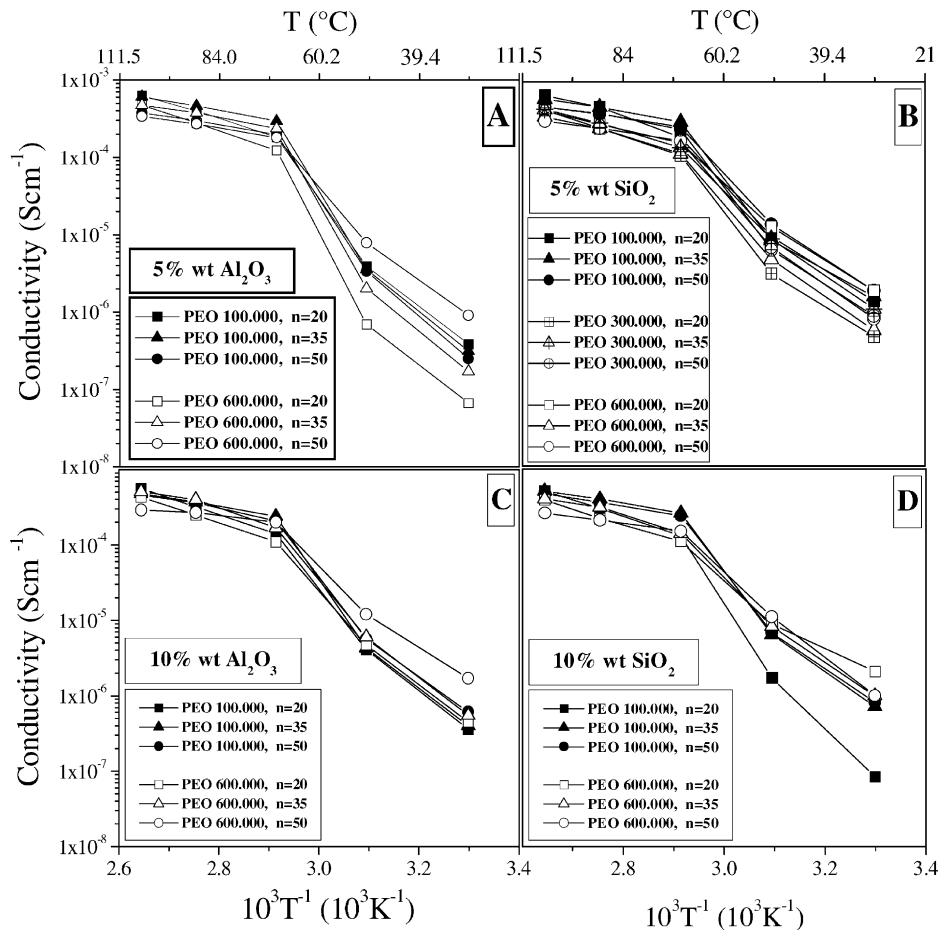


Fig. 6. Arrhenius plots of the ionic conductivity of the hot-pressed, composite,  $P(\text{EO})_n\text{LiCF}_3\text{SO}_3$  for electrolyte membranes of the Series I, II and III. Panels from A to D refer to membranes differing by the type and content of the filler, i.e. 5 wt.%  $\text{Al}_2\text{O}_3$  (panel A), 5 wt.%  $\text{SiO}_2$  (panel B), 10 wt.%  $\text{Al}_2\text{O}_3$  (panel C), and 10 wt.%  $\text{SiO}_2$  (panel D). Each panel reports the conductivity data for different PEO molecular masses (see legend) and EO/Li molar ratios (see legend). Data obtained by impedance spectroscopy.

### 3.3. Ionic conductivity

The specific ionic conductivity value,  $\sigma$ , of the hot-pressed, dry, composite, PEO-based, polymer electrolyte membranes was determined by using the following equation:

$$\sigma = \frac{t}{(d/2)^2 \pi R_i} \quad (1)$$

where  $t$ ,  $d$  and  $R_i$  represent the thickness, the diameter and the ionic resistance (bulk resistance + grain boundary resistance), respectively of the sample membrane.

The experimental error,  $\Delta\sigma$ , on conductivity was evaluated using the following equation:

$$(\Delta\sigma)^2 = \left(\frac{\partial\sigma}{\partial t}\right)^2 (\Delta t)^2 + \left(\frac{\partial\sigma}{\partial d}\right)^2 (\Delta d)^2 + \left(\frac{\partial\sigma}{\partial R_i}\right)^2 (\Delta R_i)^2 \quad (2)$$

where  $\Delta t$ ,  $\Delta d$  and  $\Delta R_i$  represent the errors associated with the thickness, the diameter and the ionic resistance of the sample membrane, respectively.

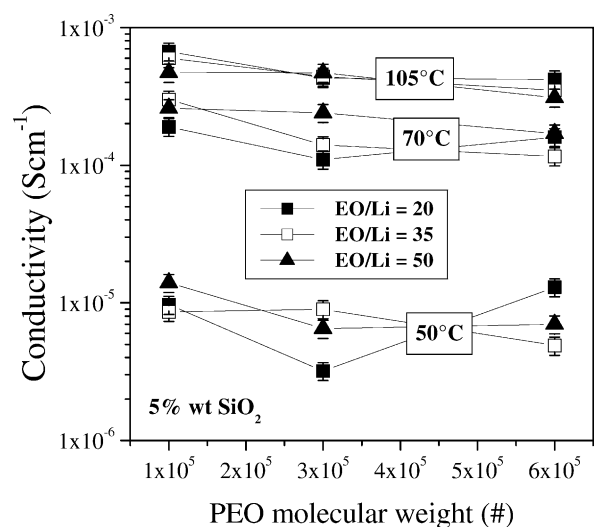


Fig. 7. Ionic conductivity vs. PEO molecular mass dependence for selected, hot-pressed, nanocomposite,  $P(\text{EO})_n\text{LiCF}_3\text{SO}_3$  membranes for Series I, II and III with 5 wt.%  $\text{SiO}_2$  as a function of EO/Li molar ratios (see legend) and temperature (see legend). Data obtained by impedance spectroscopy. The error bars for the conductivity values are also reported.

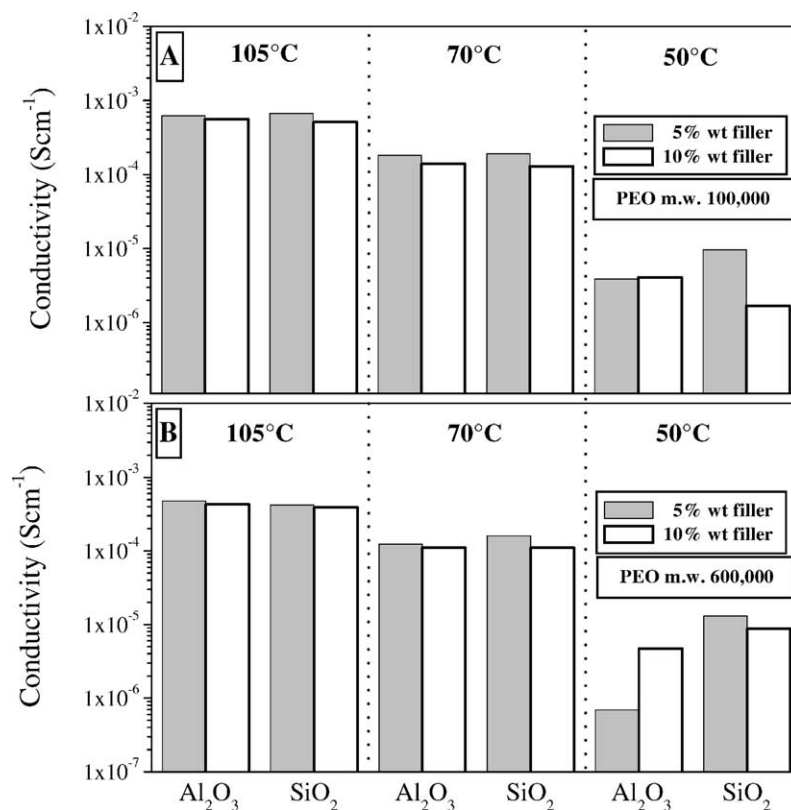


Fig. 8. Ionic conductivity of selected, hot-pressed, nanocomposite,  $\text{P}(\text{EO})_{20}\text{LiCF}_3\text{SO}_3$  for Series I and III membranes as a function of the filler type (see legend) and content (see legend), PEO molecular mass (see legend), and temperature (see legend). Panels A and B are referred to PEO molecular masses of 100,000 (panel A) and 600,000 (panel B), respectively. Data obtained by impedance spectroscopy.

The conductivity values of the membranes in the Series I, II and III, determined over the 105–30 °C temperature range, are reported in Table 2. Fig. 6 shows the temperature dependence of the ionic conductivity of  $\text{P}(\text{EO})_n\text{LiCF}_3\text{SO}_3$  composite membranes differing by the type and the content of the ceramic filler, i.e. 5 wt.%  $\text{Al}_2\text{O}_3$  (panel A), 5 wt.%  $\text{SiO}_2$  (panel B), 10 wt.%  $\text{Al}_2\text{O}_3$  (panel C), and 10 wt.%  $\text{SiO}_2$  (panel D). Each panel reports the conductivity data for different PEO molecular masses (see legend) and for different EO/Li molar ratios (see legend). All polymer electrolytes investigated exhibited a similar trend, namely a non-linear enhancement of the conductivity by increasing the temperature. Two quasi-linear slope regions with a knee around 70 °C, as typical of the generality of PEO-based polymer electrolytes [1,4] are observed. The slope of the Arrhenius plots is related to the activation energy,  $E_{\text{act}}$ , for ionic transport. The change in slope around 70 °C reflects the well-known change in the conduction mechanism associated with the PEO crystalline–amorphous transition phase.

Fig. 7 compares the conductivity values of selected  $\text{P}(\text{EO})_n\text{LiCF}_3\text{SO}_3$ : 5 wt.%  $\text{SiO}_2$  membrane samples of the Series I, II and III. A general, slight increase of the conductivity is observed by decreasing the PEO molecular weight. This behavior is due to the progressive decrease in viscosity as the PEO molecular mass decreases which in turn results in enhancement of the mobility of the  $\text{Li}^+$  ions

[18,19]. In fact, even a moderate increase of the molecular weight leads to a remarkable enhancement of the flow index (e.g. the viscosity) of the polymer [20]. An anomalous trend, i.e. a surprisingly high conductivity at 50 °C is shown by the membrane samples using PEO of 600,000 molecular mass with an EO/Li composition equal to 20 (solid square markers). This may very reasonably be attributed to hysteresis phenomena [4] of the tested samples. The results reported in Fig. 7 clearly show that, at temperatures of interest for application in lithium polymer batteries at and above 70 °C, the ionic conductivity of the solid-state electrolyte is practically independent of PEO molecular mass, at least in the 100,000–600,000 range for the systems included in the present investigation. This is of relevant practical importance since it provides the opportunity of selecting a low molecular weight PEO polymer, this in turn allowing one to carry out the hot-pressing process of the membranes under soft conditions in terms of temperature, pressure and time, this finally giving advantages in terms of power saving and safety.

In addition, Fig. 7 shows that no relevant influence of the EO/Li lithium salt concentration is observed (especially above 50 °C), at least in the EO/Li = 20–50 range for the systems included in the present investigation. The choice of an appropriate EO/Li molar ratio is important in view of applications since this parameter regulates the  $\text{Li}^+$  ion



concentration gradient in the electrolyte separator. A low EO/Li ratio (i.e. high salt concentration) might lead to excessive ion pair formation and/or the formation of  $P(EO)_nLiX$  complexes ( $n < 8$ ) having a high melting point which will significantly reduce the conductivity of the electrolyte membrane. On the other hand, a high EO/Li ratio (i.e. low salt concentration) might lead a remarkable decrease of the lithium ion concentration at electrolyte/electrode interface, thus introducing possible limitations due to concentration polarization and/or decrease in charge carriers lower conductivities. The results of Fig. 7 demonstrate that the lithium salt concentration of the electrolyte membrane can be shifted from a EO/Li ratio = 20–50 without significant loss of ionic conductivity, this allowing the choice of the best composition in terms of performance of a given battery device.

Finally, Fig. 8 illustrates the influence of the nature and of the content of the filler on the ionic conductivity of the hot-pressed, composite  $P(EO)_{20}LiCF_3SO_3$ , Series I and III electrolyte membranes for different PEO molecular masses and temperatures at a fixed EO/Li molar ratio = 20. Fig. 8 refers to membranes for PEO having molecular masses of 100,000 (panel A) and 600,000 (panel B). Two types of fillers, i.e. 5 and 10 wt.%  $Al_2O_3$  and  $SiO_2$  are compared in this figure. No practical effect is observed above 70 °C while a slight increase in conductivity is noticed for the  $SiO_2$ -based membranes at 50 °C, i.e. below the PEO crystalline–amorphous phase transition temperature. The present results reveal the important feature that transport properties at temperatures  $\geq 70$  °C are essentially independent upon the wt.% filler content. In addition to enhancing conductivities, fillers have a relevant role in promoting the mechanical stability of the electrolyte, this being a crucial advantage for practical applications.

#### 4. Conclusions

Several composite  $P(EO)_nLiCF_3SO_3$  membranes with various wt.%  $SiO_2$  or  $Al_2O_3$  fillers were prepared by hot-pressing of powder mixtures through a completely dry, solvent-free procedure. This process resulted in homogeneous membrane samples having very good mechanical properties. The influences of several factors (e.g. temperature, composition) on ionic conductivity were investigated. In particular we found the following:

1. All polymer electrolytes exhibited a similar conductivity/temperature dependence and reached the  $10^{-4} S cm^{-1}$  value at 70 °C.
2. The ionic conductivity of the hot-pressed, nanocomposite membranes is not influenced by the PEO molecular weight or by the EO/Li molar ratio, especially above 70 °C.
3. No practical effect on conductivity enhancement is observed at high filler contents, i.e. above around 5 wt.%.

#### Acknowledgements

This work has been supported by the US Army under Contract No. DAAB07-01-C-D414.

#### References

- [1] M. Armand, J.M. Chabagno, M.J. Duclot, in: P. Vashishita, J.N. Mundy, G.K. Shenoy (Eds.), *Fast Ion Transport in Solids*, Elsevier, New York, 1989.
- [2] P. Lightfoot, M.A. Metha, P.G. Bruce, *Science* 262 (1993) 883.
- [3] C.A. Vincent, B. Scrosati, *Modern batteries, An Introduction to Electrochemical Power Sources*, 2nd ed., Arnold, London, 1993.
- [4] F.M. Gray, *Polymer Electrolytes*, Royal Society of Chemistry Monographs, Cambridge, 1997.
- [5] W. Wieczorek, K. Such, H. Wycislik, J. Plochanski, *Solid State Ionics* 36 (1989) 255.
- [6] F. Capuano, F. Croce, B. Scrosati, *J. Electrochem. Soc.* 138 (1991) 1918.
- [7] M.C. Borghini, M. Mastragostino, S. Passerini, B. Scrosati, *J. Electrochem. Soc.* 142 (1995) 2118.
- [8] F. Croce, G.B. Appetecchi, L. Persi, B. Scrosati, *Nature* 394 (1998) 456.
- [9] G.B. Appetecchi, F. Croce, L. Persi, F. Ronci, B. Scrosati, *Electrochim. Acta* 45 (2000) 1481.
- [10] P.P. Prosini, S. Passerini, R. Vellone, W.H. Smyrl, *J. Power Sources* 75 (1998) 73.
- [11] G.B. Appetecchi, S. Scaccia, S. Passerini, *J. Electrochem. Soc.* 147 (2000) 4448.
- [12] G.B. Appetecchi, S. Passerini, *Electrochim. Acta* 45 (2000) 2139.
- [13] G.B. Appetecchi, F. Alessandrini, R.G. Duan, A. Arzu, S. Passerini, *J. Power Sources* 1 (2001) 4335.
- [14] G.B. Appetecchi, W. Henderson, P. Villano, M. Berrettoni, S. Passerini, *J. Electrochem. Soc.* 148 (2001) 1171.
- [15] J.R. MacDonald, *Impedance Spectroscopy*, Wiley, New York, 1987.
- [16] B.A. Boukamp, *Solid State Ionics* 18 (1986) 136.
- [17] B.A. Boukamp, *Solid State Ionics* 20 (1986) 31.
- [18] F. Croce, S.D. Broan, S. Greenbaum, S.M. Slane, M. Salomon, *Chem. Mater.* 5 (1993) 1268.
- [19] G.B. Appetecchi, F. Alessandrini, M. Carewska, T. Caruso, P.P. Prosini, S. Scaccia, S. Passerini, *J. Power Sources* 97 (2001) 790.
- [20] F.E. Bailey Jr., J.V. Koleske, *Poly(Ethylene Oxide)*, Academic Press, New York, 1976.